García Mari, E.; Gasque Albalate, M.; Gutiérrez Colomer, RP.; Ibáñez Solís, F.; González Altozano, P. (2013). A new inlet device that enhances thermal stratification during charging in a hot water storage tank. Applied Thermal Engineering. 61(2):663-669. doi:10.1016/j.applthermaleng.2013.08.023.

A new inlet device that enhance thermal stratification during charging in a hot water storage tank

García-Marí, Eugenio[1*], Gasque, María[2], Gutiérrez-Colomer, Rosa Penélope[1], Ibáñez, Federico[1], González-Altozano, Pablo[1]

Universitat Politècnica de València. Camino de Vera s/n. 46022 Valencia (Spain)

[1] Dept. Ingeniería Rural y Agroalimentaria. [2] Dept. Física Aplicada.

Abstract

Solar thermal energy systems are generally provided with a water storage tank. In this tank, thermal stratification takes place naturally, although it is considerably affected by the turbulence and mixing created by the water inflow and outflow. Consequently, thermal stratification is directly influenced by the inlet configuration. This study compares the effect of two water inlet devices in a hot water storage tank during a thermal charge process: a sintered bronze conical diffuser (SBCD) and a conventional inlet elbow (E). The evolution of the temperature recorded by the thermocouples, the 1-MIX number, as well as the thermocline evolution and other related parameters (shape, thickness and height of midpoint) are used to quantify the performance of the stratification. The results obtained show that the SBCD favours water stratification during thermal charging with both low and high flows. The evolution of the dimensionless height of the midpoint of the thermocline can be used to quantify the volume of water affected by the mixing produced by the turbulence generated by the water flow throught the inlet device.

Keywords: diffuser, thermocline, stratification, thermal energy storage

1. Introduction

Since the 1980s there has been an increasing interest to improve the performance of individual equipment components of the solar water heating systems in order to obtain higher efficiencies and

energy savings [1]. In these systems, the water is always heated by flowing through the solar collector, and it is then conducted to an energy storage device, which is generally a hot water storage tank.

In the storage tank, thermal stratification takes place naturally; the cold water remains at the bottom of the tank separated from the hot water, which flows to the top. This separation is maintained by the different densities of the hot and cold water layers. Stable thermal stratification in the water tank must be maintained in order to improve the efficiency of the thermal storage and consequently the overall performance of the solar system [2,3]. Thus, the efficiency of solar collectors is improved if the inlet water temperature is kept low and the temperature of the water to be charged is kept high.

The loss or degradation of thermal stratification in solar storage tanks is caused mainly by the mixing that occurs during the charge and discharge processes. Mixing takes place when the water inlet temperature is different from that of the stored water with which it comes into contact. Therefore, designing water inlet devices to distribute the flow uniformly improves the performance of thermal storage tanks by restraining the mixing induced by water inflow [4-8].

A thermal stratified tank can be characterised by its thermocline, the region of steepest temperature gradient separating the hot and cold fluid region in the tank [9]. Parameters related to the thermocline, such as its thickness or the dimensionless height of its midpoint, may also be used to assess the degree of stratification in a tank, and to this end, the thickness of the thermocline region has been employed in many studies [6,8,10,11].

In addition to the thermocline, other indices have been used to quantify the stratification efficiency of thermal energy storage tanks. Although none are widely accepted [12], the MIX number, an index proposed by Davidson et al. [13] and modified by Andersen et al. [14] has been employed in recent research [15,16].

This paper describes experiments which analyze the effect of a sintered bronze conical diffuser (SBCD) and a conventional inlet elbow (E) on thermal stratification during the charge process in a

solar storage tank. Different hot water flow rates were tested, and results compare the performance of the two inlet devices. The indices used to evaluate the degree of thermal stratification were the graphic temperature profiles, the evolution of the thermocline, its thickness and the height of its midpoint, as well as the 1-MIX number.

2. Materials and methods

The experimental trials were conducted with a cylindrical hot water storage tank of 905 L capacity (800 mm inner diameter and 1800 mm height). The side-walls, top and bottom were covered with a 50-mm thick layer of insulating material (fiber glass). A conventional inlet elbow (E) and a sintered bronze conical diffuser (SBCD) (Fig. 1 and Fig. 2) were arranged independently at the top of the tank, symmetrically with regard to the vertical axis. The SBCD was a muffler normally used on valve exhaust ports, made by Ingersoll-Rand Company and formed by bronze microspheres joined together by pressure (sintered) forming a porous wall (40 μm), allowing water flow across its entire surface. 93% of the flow entered through the sidewall of the SBCD while 7% entered through the flat base. The average velocity of water coming out through the SBCD was around 21% of the average velocity through the elbow.

In order to record the water temperature in the tank, 12 type T (Class 1) thermocouples (TC) were distributed uniformly and symmetrically along the vertical axis of the tank (150 mm apart and 75 mm from both the top and the bottom of the tank). Similarly, two TC were used to register the water inlet and outlet temperatures during the charge process.

Two thermostated tanks, with hot and cold water respectively, were used to ensure a constant temperature of the inlet water supply to the storage tank. A fourth tank was also needed to store the output water from the experimental tank during the trials. The water flow was measured at the tank entrance using an electromagnetic flowmeter (Endress Hauser mod. Promag 53H08 DN8 error<±0.2%). Constant flow was guaranteed by a pump with a variable speed drive (Altivar 61) controlled using the flowmeter signal as an input. Fig.3 illustrates the experimental setup.

The signal of each sensor was registered using the data acquisition system Compact DAQ 9178 of National Instruments, with a NI-9213 module (16-ch, 24 bits) for the thermocouple signal conditioning and acquisition, and a NI-9208 module (16-ch mA, 24 bits) for the flowmeter signal acquisition. The signals were captured, displayed and recorded by software compiled in Labview (National Instruments) with a 0.1 Hz frequency.

TC temperatures with all the acquisition system were calibrated against a PT100 (error <±0.1%).

The installation was automatically controlled and thus ensured the repeatability of the trials. This was verified by comparing three identical trials performed in the same conditions, (data not shown); the maximum temperature difference between TC for the different tests was always less than 2%.

Six thermal charging tests were carried out with the two inlet devices: the elbow (E) and the sintered bronze conical diffuser (SBCD), at three water flow rates: high (H, 16 L/min), medium (M, 10 L/min) and low (L, 6 L/min) (Table 1). The water tank temperature was 20±0.2 °C at the start of each trial (T_c). In all cases, a constant flow rate was injected from the tank thermostated to 52±0.2 °C (T_h) until 80% of the total storage tank volume was replaced. The duration of the charge is expressed as dimensionless time, determined as follows:

$$t^* = \frac{Flow\left(L/s\right) \times time\,(s)}{Tank\ volume\,(L)} \qquad (1)$$

The data recorded were treated using Matlab-implemented programmes, which also provided a graphic representation of the results [17].

The performance of the two inlet devices on stratification during thermal charging of the tank was assessed and quantified by means of several analysis and indexes.

First, the evolution of the temperatures was recorded by the 12 TC and 3 of them, placed at representative locations in the tank, were selected for comparison: TC1 (top of the tank), TC6 (middle), and TC11 (bottom). The MIX number and the graphic evolution of the temperature profile (thermocline) were also analyzed.

The MIX number proposed by Davidson et al. [13] and modified by Andersen et al. [14] is based on determining the momentum of energy contained in the different layers of the tank through the length of its vertical axis. This momentum is obtained as a product of the energy in one layer by its distance from the base of the tank. The momentum of energy contained throughout the tank is the sum of the momenta of its layers.

The Andersen MIX number, as indicated in Eq. (2), is obtained from the momenta of the energy calculated for the experimental tank (M_{exp}), for a perfectly stratified tank (M_{est}), and for a completely mixed tank (M_{mix}). The theoretical stratified and mixed storages are determined at each instant and therefore have the same energy content as the experimental tank at any time.

$$MIX = \frac{M_{est} - M_{exp}}{M_{est} - M_{mix}} \quad (2)$$

The 1-MIX value is proposed as a stratification index [12], and it ranges from 1 for a perfectly stratified tank to 0 for a fully mixed tank. In this study, the evolution of the 1-MIX number was analyzed for the two inlet devices and for the different flows.

Besides, to quantify the performance of the stratification in this thermal energy storage tank with each inlet device, the evolution of the temperature profile (thermocline) during charging was studied following the procedure described by Waluyo and Majid [18].

Thus, a Four Parameter Sigmoid (FPS) function was fitted to the temperature distribution profile using Eq. (3):

$$T = T_c + \frac{T_h - T_c}{1 + e^{\frac{C-X}{S}}} \quad (3)$$

The FPS function relates temperature distribution to one variable X and four parameters: T_c (cold water tank temperature at the start of each trial, °C), T_h (hot water inlet temperature, °C), C (dimensionless height of the midpoint of the thermocline), and S, a parameter related to the slope of the change between hot and cold water temperatures.

The variable X expresses the dimensionless height of the temperature sensors (x/H_e), where x (m) is the height of the temperature sensors, and H_e (m) is the height of the water content in the tank (1.8 m). T represents the water temperature (°C) in the tank at the dimensionless height X.

Parameters T_c, T_h, C and S were obtained by fitting the FPS function to the temperature profile every 10 seconds throughout the entire charge process using the lsqcurvefit Matlab function. Additionally, the evolutions of the parameter C (dimensionless height of the midpoint of the thermocline) as well as the thermocline thickness, with the higher and lower flows, were also evaluated.

Thermocline thickness can be obtained from the FPS function by rearranging Eq. (3) as follows:

$$\frac{T - T_c}{T_h - T_c} = \frac{1}{1 + e^{\frac{C-X}{S}}} \tag{4}$$

and considering the dimensionless cut-off temperature $\Theta = (T-T_c)/(T_h-T_c)$ [19], describing the limit points of the thermocline thickness, the Eq. (4) can be written as:

$$\Theta = \frac{1}{1 + e^{\frac{C-X}{S}}} \tag{5}$$

where the distance from C to X expresses the half-thickness of the thermocline, determined as follows:

$$C - X = S \cdot \ln\left(\frac{1}{\Theta} - 1\right) \tag{6}$$

Hence, the thermocline thickness L_{Tc} is defined as:

$$L_{Tc} = 2 \cdot S \cdot \ln\left(\frac{1}{\Theta} - 1\right) \tag{7}$$

This equation was used to determine the thermocline thickness for a predetermined value of Θ. Conceptually, the dimensionless cut-off ratio Θ values are in the range of 0 to 0.5 covering minimum and maximum thermocline thicknesses. The value Θ=0 indicates that the upper and lower limits of the thermocline region are located at T_c and T_h; therefore, a maximum thickness is obtained. With

Θ=0.5, the limit points are at the midpoint of the thermocline region, and the resulting value for thickness is zero. In this study the value Θ = 0.1 was used.

3. Results and discussion

Fig. 4 shows the evolution of the temperature for the thermocouples TC1, TC6 and TC11, depending on dimensionless time, during the thermal charge process for the trials described in Table 1.

At the end of the charge period, the temperatures in the top and the middle part of the tank were lower with the elbow than with the SBCD, indicating a greater degree of mixing during thermal charging. This effect was more pronounced when the input flow was higher and it was especially noticeable in the top of the tank (values registered by TC1). In the case of the elbow, the temperature rose more slowly as the flow increased but it did not reach the value of the inlet temperature, even by the end of the charge period. This demonstrates the destratifying effect produced by a higher flow as it has been reported by other experimental [7] and numerical [20] studies. In contrast, in the case of the SBCD, and in both the top and the middle region, the flow did not significantly affect stratification, and the temperatures were the same for the three flows as the charge process was finishing. For the elbow, the temperatures recorded by the TC6 (middle region of the tank) showed that the increase in temperature started first; this result, together with the smaller slopes observed, indicated a greater degree of mixing. Likewise, in the lower region of the tank (TC11), the increase in temperature caused the hot water to leave the tank first and thus the efficiency of the installation was affected negatively. For the higher flow rate (E-H) the increase in temperature took place in a dimensionless time of 0.65 and for the lower flow rate (E-L), 0.8. During this charge period (80% of the tank volume replaced), no increase in the outlet temperature was observed in the case of SBCD. The results show that a higher thermal stratification was achieved using the inlet SBCD for the three flows, and this high degree of stratification was constant throughout the charge period studied. In contrast, the loss of thermal stratification was largely influenced by the flow in the case of the elbow.

The fluctuations in the temperature due to the turbulence created by the water inflow were greater when water came through the elbow, being higher at the higher flow (E-H>E-M>E-L). Moreover, they were virtually negligible when the water entered through the SBCD. The fluctuations in this signal indicate the degree of mixing in the tank due to the hot water inflow, and are related to the speed at which the temperature in the first thermocouple increased. The lower the fluctuations, the faster this temperature increased, indicating less mixing of the water inside the tank.

In view of these results, it seems that the evolution of the temperatures registered by the thermocouples can be used to qualitatively compare the effect of different inlet devices on thermal energy storage tanks.

Fig. 5 shows the evolution of the 1-MIX number for the experiments specified in Table 1. In all cases a high degree of stratification is observed during the charge period studied (80%) since the calculated values for the index were above 0.9. In the case of SBCD, the 1-MIX number was similar for the three flows, and their values were about 0.97 until the end of the charge period. In the case of the elbow, on the other hand, there were differences among the three flows. For the lower inlet flow, the values of the 1-MIX number were similar to those calculated for the SBCD. However, for the higher flow the values of the index remained around 0.94 and diminished to 0.90 at the end of the charge period considered. The greatest variability in the 1-MIX index for the elbow with high flow indicates more turbulence in the water tank. Thus, a greater destratifying effect is observed with the highest flow. Nonetheless, the flow had little effect on the mixing and therefore on stratification when the water entered through the SBCD.

The differences observed in the 1-MIX number were in accordance with the variations in the temperature profiles (Fig. 4). However, this index appeared hardly sensitive to the destratification produced during thermal charging given the slight differences among the calculated values from the different trials. Thus, in this work another parameter was considered to check the degree of thermal stratification during charging: the analysis of the thermocline.

Fig. 6 depicts the function of the thermocline determined by fitting Eq. (3) for the temperature profile corresponding to dimensionless filling times of 0.2 and 0.6 for both inlet devices and with the high (H) and low (L) flows (Table 1). In the case of the inlet elbow and for dimensionless time 0.2, the 3 TC at the top of the tank recorded temperatures lower than the inlet water temperature. This indicates that a greater degree of mixing took place at the top of the tank. This effect was more pronounced with the high flow. As the charge progresses, up to 0.6, this effect was attenuated although the inlet water temperature was not reached. In contrast, with the SBCD, temperatures at the top of the tank were close to the water inlet temperature during the thermal charge period up to 0.6, regardless of the flow employed. Thus, a high degree of thermal stratification was achieved. The slope of the thermocline, and therefore its thickness, was lower in the case of inflow through the SBCD for all the flows tested. In the case of the inlet elbow, a greater thermocline slope can be observed with higher flows. In contrast, with the inlet SBCD the thermocline curves were similar for all the flows.

These results show again the lower degree of thermal destratification produced by the inlet SBCD compared to the inlet elbow during the tank charge process. The effect of the flow was hardly noticeable in the case of the SBCD and it negatively affected stratification in the case of the elbow (greater mixing when there was a higher flow).

As reported by Majid and Waluyo [21], the adjusted function resulted in a clearer separation of the temperature in the region of the asymptotes curve, and the profile of water temperature determined by the function was clearly defined.

As illustrated in Fig. 6, the values of TC remained constant in all trials until approximately 60% of the charging with the elbow and higher flow due to the diffusion of the thermocline region and in accordance with the evolution of the temperature in the lower region of the tank (Fig. 4). However, T_h increased during the charge cycle due to the incoming supply of hotter water through the tank inlet. This increment was higher for the higher flows and much more noticeable with the inlet elbow,

being practically negligible with the SBCD indicating that there was less mixing in this case. Similar effects were also found [21-23] in experiments performed with chilled-water tanks.

The evolution of the dimensionless height of the midpoint of the thermocline (parameter C in Eq. (3)), determined by fitting the FPS function, is given in Fig. 7 depending on the dimensionless charging time for the two inlet devices with the higher and lower flows. In all cases, the parameter C decreased linearly with the time of charge, indicating that thermocline position moved downwards from the top to the bottom of the tank during the charge cycle.

In an ideal case of a tank with a constant section, there is an inverse linear relationship between the dimensionless height of the midpoint and the dimensionless time throughout the charge process. When there was less mixing (inlets SBCD and E-L) and the conduction phenomena prevailed over the mixing, this relationship followed an ideal straight line of slope -1 (dashed line in Fig. 7). Nevertheless, when turbulence produced a greater mixing (E-H), the evolution of this relationship deviated from the ideal straight line due to the mixing near the inlet produced during thermal charging in a volume approximately equal to the dimensionless height difference (12% in this case). As other studies have reported [9, 23, 24], the extent of this mixing, directly related to the diffuser design, primarily influenced the shape of the thermocline (Fig. 6).

Parameter C is not sensitive to discriminate degrees of stratification but it is useful to indicate the progression of the thermocline which results from the mixing and destratification in the tank inlet (Fig. 6, E-H). Likewise, this parameter can be used to determine the water volume affected by the mixing produced by the inlet water.

Fig. 8 shows the evolution of the dimensionless thermocline thickness for the two inlet devices and with the high (H) and low (L) flows. The oscillations in the thermocline thickness were due to the temperature being measured at discrete points in the tank determined by the position of the thermocouples. The trend reflects how the thermocline thickness increased progressively with charging time, and was lower for the SBCD than for the inlet elbow indicating better stratification when water entered through the SBCD. With the inlet elbow, the higher flow rates resulted in an

increase in the thickness of the thermocline region, indicating a greater degree of mixing, as many authors have reported [11, 21, 23]. However, when the water entered through the SBCD, the evolution of the thermocline thickness was similar for high and low flows. In both cases, the thermocline thickness was smaller than when the water entered through the elbow at the lower flow.

From the study of both the thickness and the evolution of the dimensionless height of the midpoint of the thermocline during thermal charging, the use of SBCD as a water inlet device appears to favour the thermal stratification at all the flow rates.

4. Conclusions

Experiments were designed to examine thermal stratification during thermal charging in a solar storage tank. To this end, two water inlet devices were tested at three different flow rates. By analyzing the values for the temperature profiles in the different experiments, it was possible to compare the degree of mixing occurring in the tank water for the different trials. However, this comparison could only be qualitative.

The 1-MIX index gives a quantitative assessment of thermal stratification and shows that a greater degree of stratification is reached when the SBCD is used as an inlet device, while there are no significant differences for the three flows tested. In contrast, with the inlet elbow, a greater flow translates into a greater degree of water mixing during thermal charging of the tank.

The analysis of the indices related to the thermocline (shape, thickness, and height of the midpoint) confirms the greater degree of stratification obtained using the SBCD as an inlet device during the thermal charging of the tank at a constant temperature. The evolution of the dimensionless height of the midpoint of the thermocline can be used to quantify the volume of water affected by the mixing produced by the turbulence generated by the inlet device and the water flow.

In conclusion, the results obtained with the stratification indexes analyzed in this study demonstrate that the use of the SBCD for the hot water inlet favours thermal stratification of the water, regardless of the flow tested.

Acknowledgements

This research was supported by the *Plan Nacional de I+D+i del Ministerio de Ciencia e Innovación* (ENE2009-13376). The authors would like to thank L.H. Sanchis for his valuable and constructive suggestions during the planning and development of this research and Debra Westall for revising the manuscript.

References

[1] R. Shukla, K. Sumathy, P. Erickson, J. Gong, Recent advances in the solar water heating systems: A review, Renew. Sust. Energy Rew. 19 (2013) 173-190.

[2] C. Cristofari, G. Notton, P. Poggi, A. Louche, Influence of the flow rate and the tank stratification degree on the performances of a solar flat-plate collector, Int. J. Thermal Sci. 42 (2003) 455-469.

[3] U. Jordan, S. Furbo, Thermal stratification in small solar domestic storage tanks caused by draw-offs, Sol. Energy 78 (2005) 291-300.

[4] L.J. Shah, S. Furbo, Entrance effects in solar storage tanks, Sol. Energy 75 (2003) 337-348.

[5] M.S. Shin, H.S. Kim, D.S. Jang, S.N. Lee, Y.S. Lee, H.G. Yoon, Numerical and experimental study on the design of a stratified thermal storage system, Appl. Therm. Eng. 24 (2004) 17-27.

[6] W.P. Bahnfleth, J. Song, Constant flow rate charging characteristics of a full-scale stratified chilled water storage tank with double-ring slotted pipe diffusers, Appl. Therm. Eng. 25 (2005) 3067-3082.

[7] A.A. Hegazy, Effect of inlet design on the performance of storage-type domestic electrical water heaters, Appl. Energy 84 (2007) 1338-1355.

[8] J.D. Chung, S.H. Cho, C.S. Tae, H. Yoo, The effect of diffuser configuration on thermal stratification in a rectangular storage tank, Renew. Energy 33 (2008) 2236-2245.

[9] Y.H. Zurigat, A.J. Ghajar, Heat transfer and stratification in sensible heat storage systems, in: I. Dincer, M.A. Rosen (Eds.), Thermal energy storage. Systems and applications, John Wiley & Sons, New York, USA, 2002, pp. 259-301.

[10] A. Musser, W.P. Bahnfleth, Evolution of temperature distribution in a full-scale stratified chilled-water storage tank with radial diffusers, ASHRAE Trans. 104 part 1A (1998) 55-67.

[11] M. Walmsley, M. Atkins, J. Linder, J. Neale, Thermocline movement dynamics and thermocline growth in stratified tanks for heat storage, Chem. Eng. Trans. 21 (2010) 991-996.

[12] M.Y. Haller, C.A. Cruisckshank, W. Streicher, S.J. Harrison, E. Andersen, S. Furbo, Methods to determine stratification efficiency of thermal energy storage processes. Review and theoretical comparison, Sol. Energy 83 (2009) 1847-1860.

[13] J.H. Davidson, D.A. Adams, J.A. Miller, A coefficient to characterize mixing in solar water storage tanks, J. Sol. Energy Eng. 116 (1994) 94-99.

[14] E. Andersen, S. Furbo, J. Fan, Multilayer fabric stratification pipes for solar tanks, Sol. Energy 81 (2007) 1219-1226.

[15] N. Gopalakrishnan, S. Srinivasa Murthy, Mixed convective flow and thermal stratification in hot water storage tanks during discharging mode, Appl. Sol. Energy 45 (2009) 254-261.

[16] E. Oró, A. Castell, J. Chiu, V. Martin, L.F. Cabeza, Stratification analysis in packed bed thermal energy storage systems, Appl. Energy 109 (2013) 476-487.

[17] Matlab. Users' manual version 7.4.0 R2007a, The MathWorks Inc., Natick, MA, USA, 2007.

[18] J. Waluyo, M.A.A. Majid, Temperature profile and thermocline thickness evolution of stratified thermal energy storage tank, Int. J. Mech. and Mechatron. Eng. 10 (2010) 7-12.

[19] A. Musser, W.P Bahnfleth, Field-measured performance of four full-scale cylindrical stratified chilled-water thermal storage tanks, ASHRAE Trans. 105(2) (1999) 218-230.

[20] W. Yaïci, M. Ghorab, E. Entchev, S. Hayden, Three-dimensional unsteady CFD simulations of a thermal storage tank performance for optimum design, Appl. Thermal Eng. (2013) doi: 10.1016/j.applthermaleng.2013.07.001.

[21] M.A.A. Majid, J. Waluyo, Thermocline thickness evaluation on stratified thermal energy storage tank of co-generated district cooling plant, J. Energy Power Eng. 4 (2010) 28-33.

[22] J.E.B. Nelson, A.R. Balakrishnan, S. Srinvasa Murthy, Experiments on stratified chilled-water tanks, Int. J. Refrig. 22 (1999) 216-234.

[23] M.A. Karim, Experimental investigation of a stratified chilled-water thermal storage system, Appl. Thermal Eng. 31 (2011) 1853-1860.

[24] M.R.W. Walmsley, M.J. Atkins, J. Riley, Thermocline management of stratified tanks for heat storage, Chem. Eng. Trans. 18 (2009) 231-236.

Nomenclature

C	Dimensionless height of the midpoint of the thermocline
E	Elbow
FPS	Four Parameters Sigmoid function
H	High flow (L/min)
H_e	Height of the water content in the tank (m)
L (L/min)	Low flow
L_{Tc}	Thermocline thickness
M (L/min)	Medium flow
M_{est}	Momentum of the energy calculated for a perfectly stratified tank
M_{exp}	Momentum of the energy calculated for the experimental tank
M_{mix}	Momentum of the energy calculated for a completely mixed tank
MIX	MIX number

S	Dimensionless parameter related to the slope of the change between hot and cold water temperatures
SBCD	Sintered Bronze Conical Diffuser
t^*	Dimensionless time
T (°C)	Water temperature in the tank
T_c (°C)	Cold water tank temperature at the start of each trial
T_h (°C)	Hot water inlet temperature
TC	Thermocouple
x (m)	Height of the temperature sensors
X	Dimensionless height of the temperature sensors

Greek letters

Θ	Dimensionless cut-off temperature

Figure captions

Fig. 1. Inlet devices compared in this study. Left: conventional inlet elbow (E). Right: sintered bronze conical diffuser (SBCD).

Fig. 2. Geometry and dimensions (in mm) of both inlet devices.

Fig. 3. Experimental setup.

Fig. 4. Temperature registered by the thermocouples TC1, TC6 and TC11 during thermal charging using the inlet elbow (E) and the sintered bronze conical diffuser (SBCD) for high (H), medium (M) and low (L) flows.

Fig. 5. Evolution of 1-MIX number during thermal charging with the inlet elbow (E) and the sintered bronze conical diffuser (SBCD) for high (H), medium (M) and low (L) flows.

Fig. 6. Thermoclines fitted function at dimensionless time t^* = 0.2 (upper) and t^* = 0.6 (lower) during thermal charging using the inlet elbow (E) and the sintered bronze conical diffuser (SBCD) for high (H, 16 L/h) and low (L, 6 L/h) flows.

Fig. 7. Evolution of the dimensionless height of midpoint of thermocline during thermal charging.

Fig. 8. Dimensionless thickness of the thermoclines versus dimensionless time during thermal charging for the inlet elbow (E) and the sintered bronze conical diffuser (SBCD) with high (H, 16 L/h) and low (L, 6 L/h) flows.

Highlights

(1) It is proposed a new inlet device that improves thermal stratification.
(2) The new inlet device is compared against a conventional one during charging.
(3) 1-MIX num. and various stratification indices related to thermocline are applied.
(4) Height of midpoint of thermocline allow quantify volume of water affected by mixing.
(5) The new inlet device enhanced water stratification at all the flow rates tested.

Figure 1

Figure 2

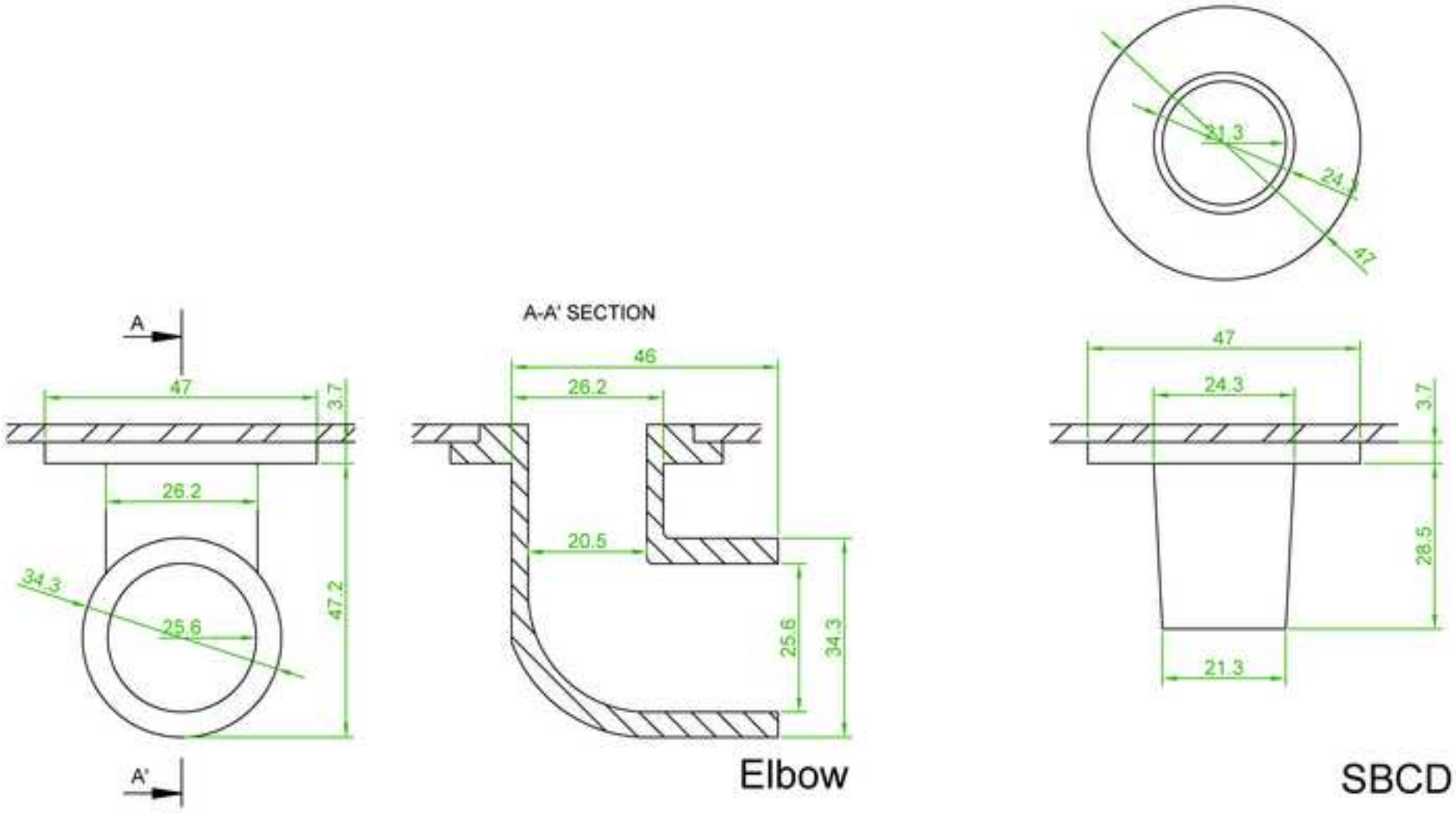

Figure 3

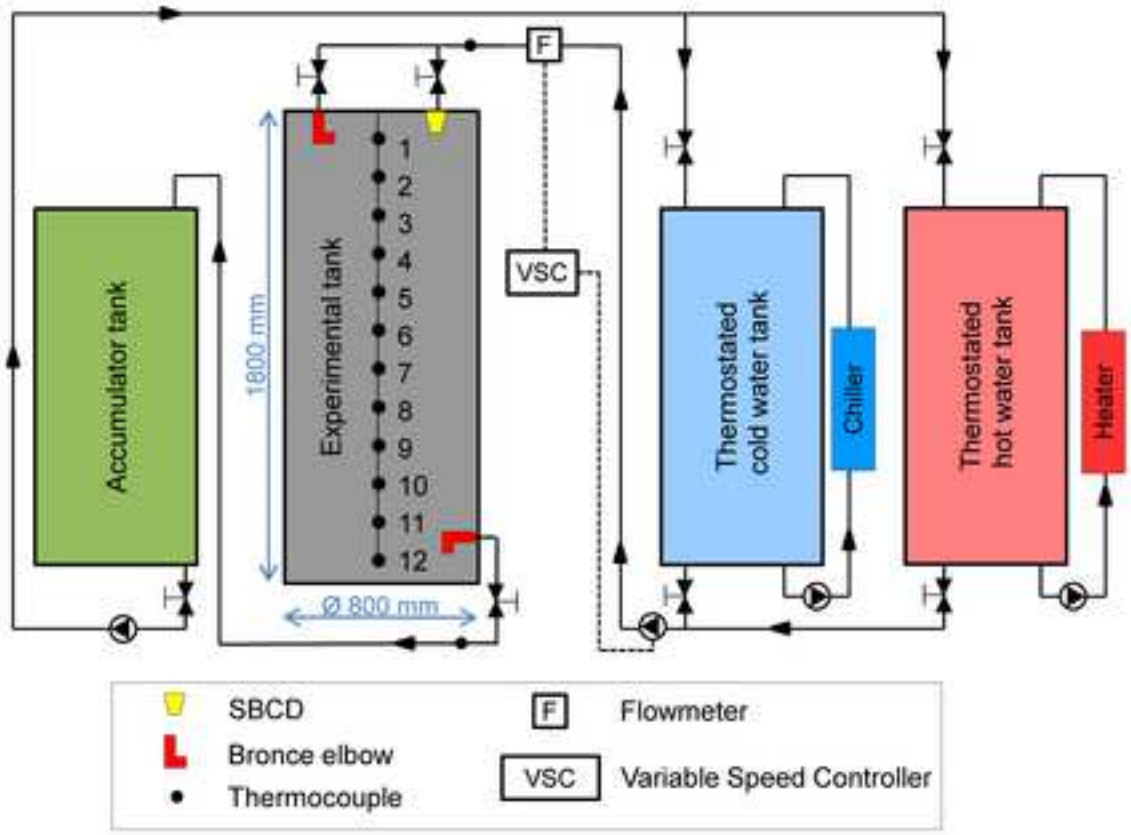

Figure 4

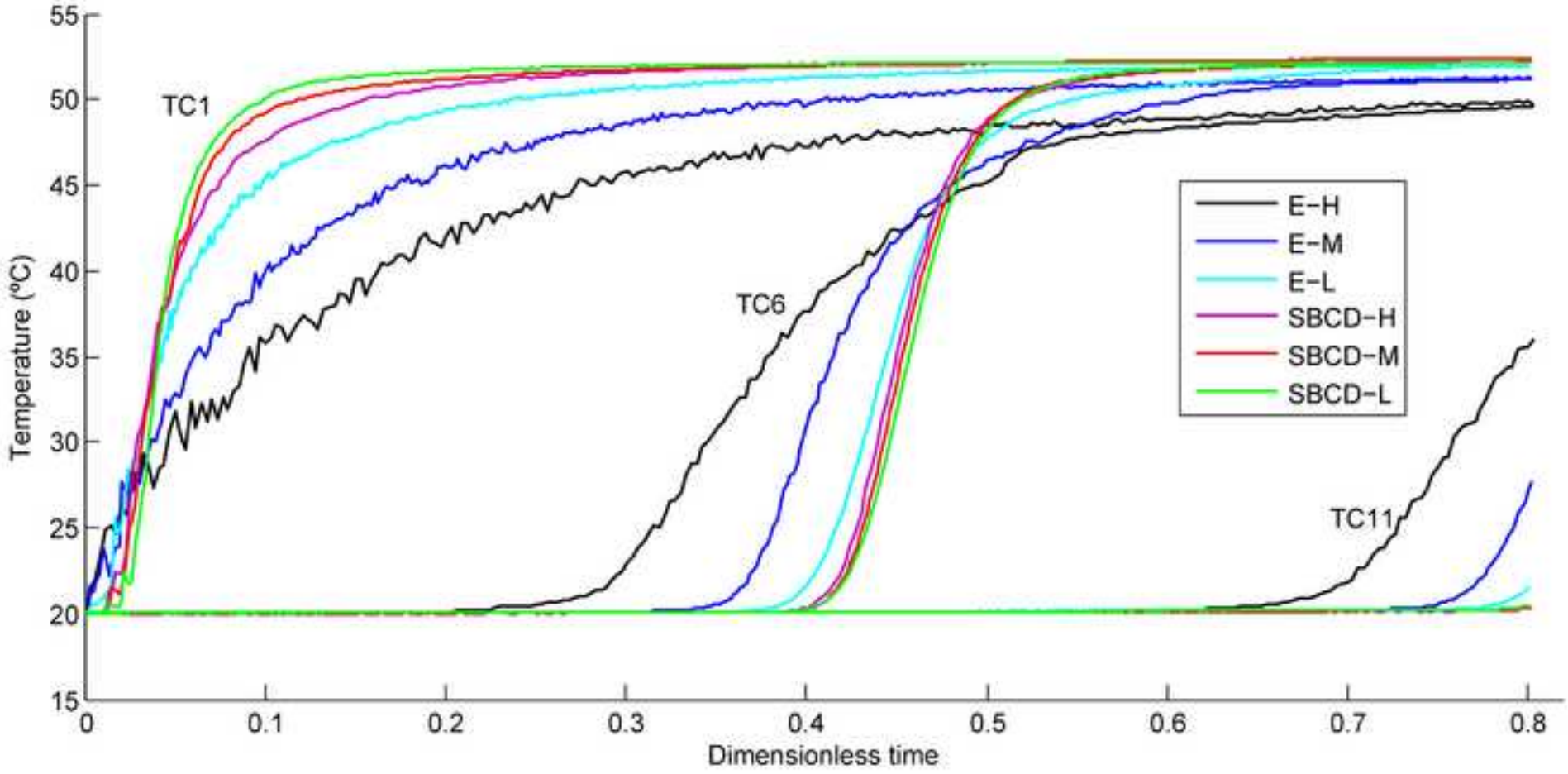

Figure 5

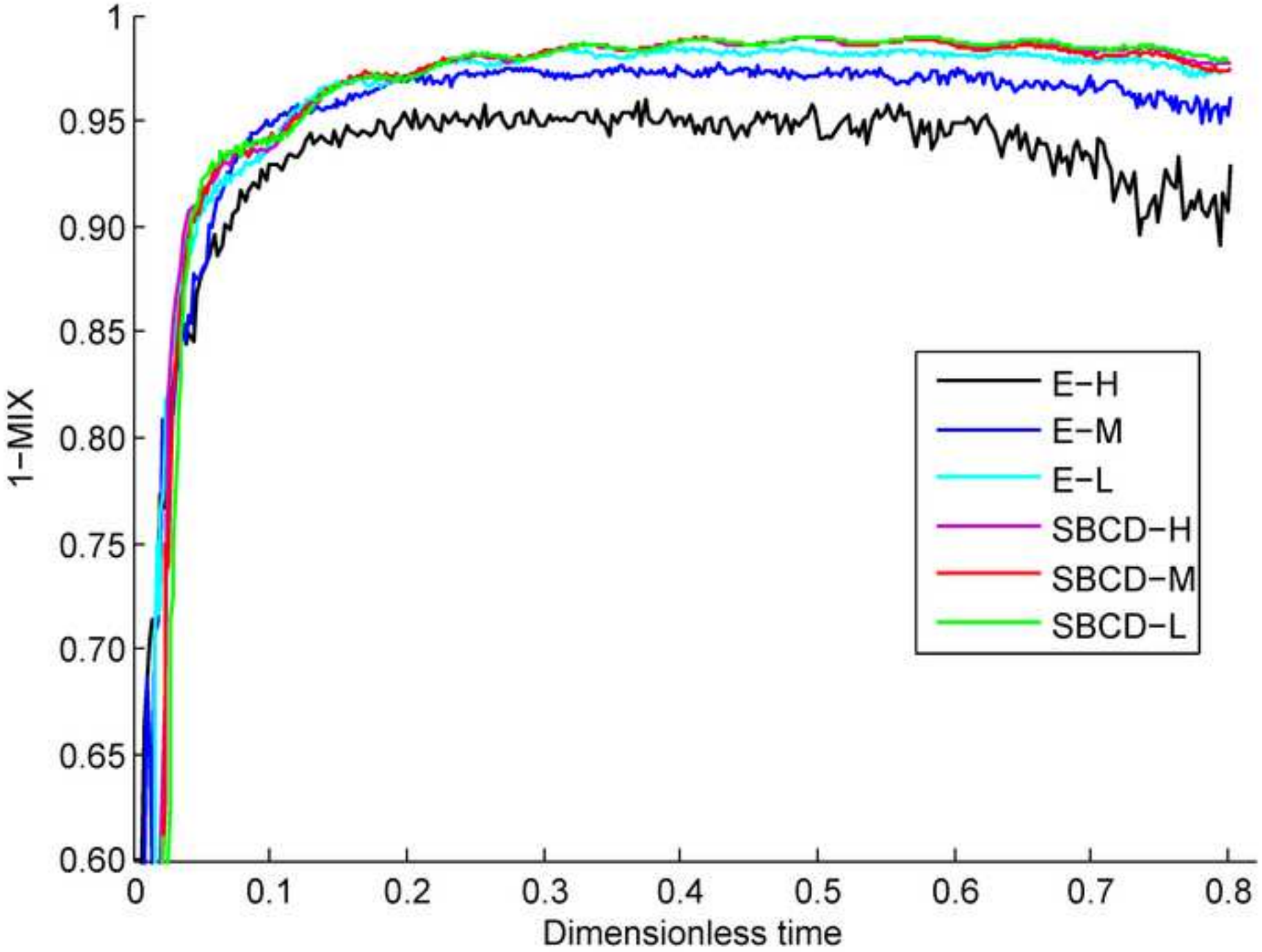

Figure 6

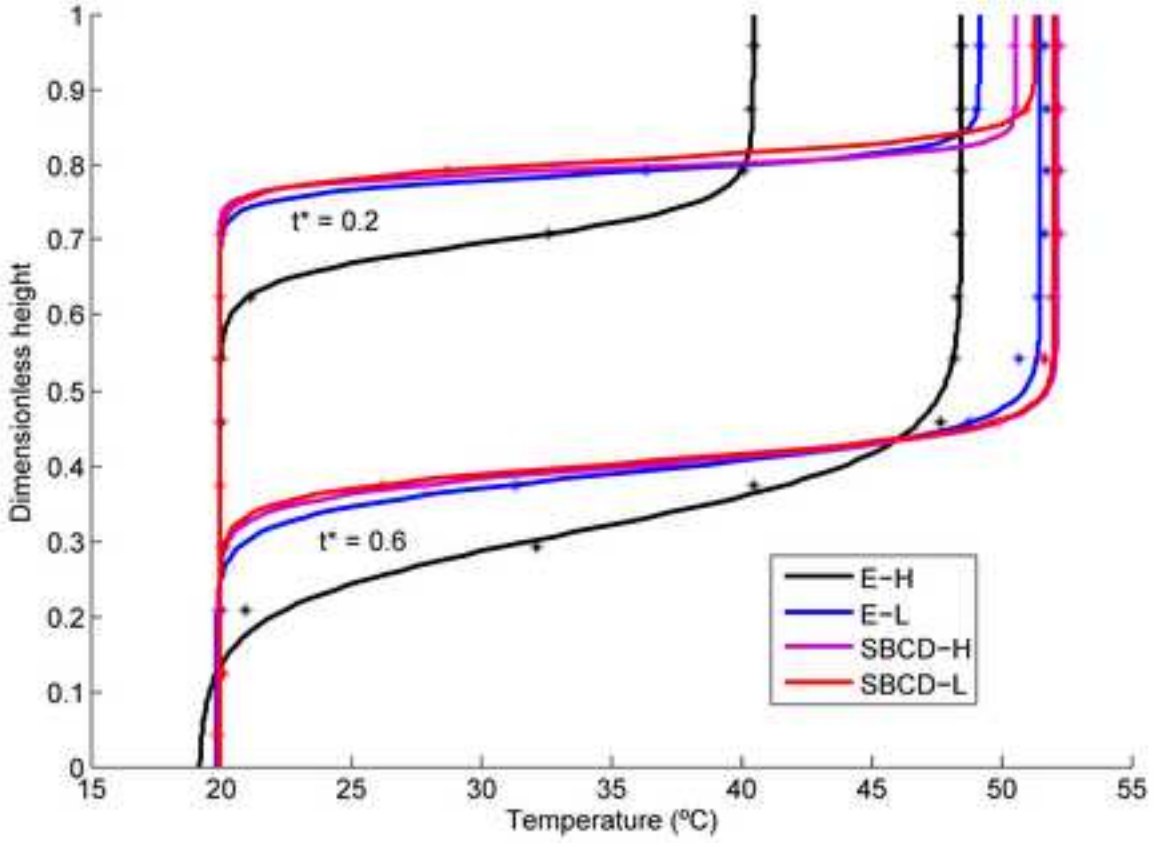
Dimensionless height
Temperature (°C)
t* = 0.2
t* = 0.6
E-H
E-L
SBCD-H
SBCD-L
0
0.1
0.2
0.3
0.4
0.5
0.6
0.7
0.8
0.9
1
15
20
25
30
35
40
45
50
55

Figure 7

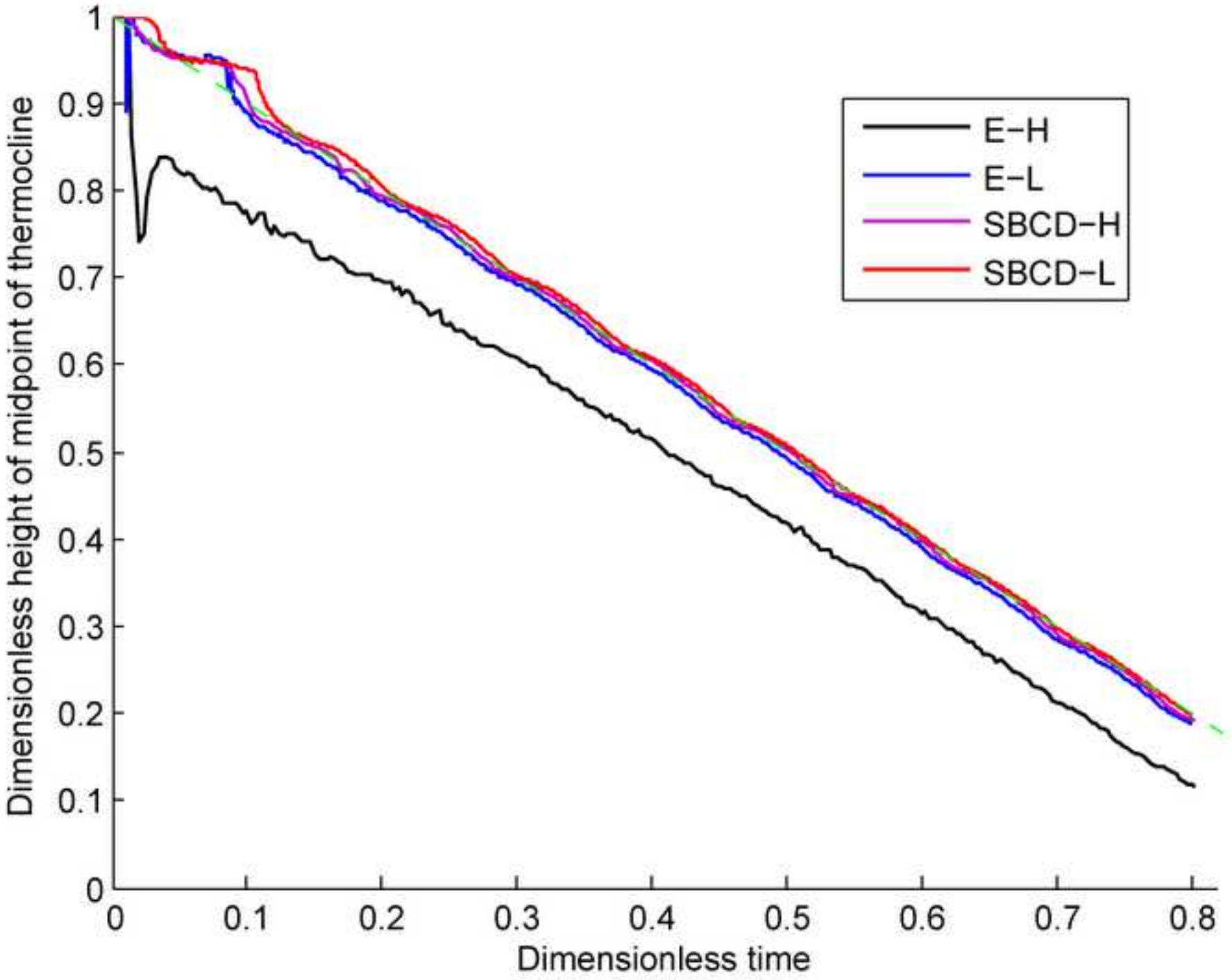

Figure 8